# A Deep Learning Method to Detect Atrial Fibrillation Based on Continuous Wavelet Transform

Ziqian Wu, Xujian Feng and Cuiwei Yang*

***Abstract*— Atrial fibrillation (AF) is one of the most common arrhythmias. The automatic AF detection is of great clinical significance but at the same time it remains a big problem to researchers. In this study, a novel deep learning method to detect AF was proposed. For a 10 s length single lead electrocardiogram (ECG) signal, the continuous wavelet transform (CWT) was used to obtain the wavelet coefficient matrix, and then a convolutional neural network (CNN) with a specific architecture was trained to discriminate the rhythm of the signal. The ECG data in multiple databases were divided into 4 classes according to the rhythm annotation: normal sinus rhythm (NSR), atrial fibrillation (AF), other types of arrhythmia except AF (OTHER), and noise signal (NOISE). The method was evaluated using three different wavelet bases. The experiment showed promising results when using a Morlet wavelet, with an overall accuracy of 97.56%, an average sensitivity of 97.56%, an average specificity of 99.19%. Besides, the area under curve (AUC) value is 0.9983, which showed that the proposed method was effective for detecting AF.**

## I. INTRODUCTION

Atrial fibrillation (AF) is a common arrhythmia with a 0.5% incident rate among the world population. What is more, the incident rate will increase significantly with the increase of age [1]. According to statistics, there are about 10 million patients with AF in China, accounting for 0.7% of China's total population [2]. In developed countries, patients with AF account for a larger proportion of the total population than in the developing countries due to the high proportion of the aging population. For example, 2% of the whole population of Europe suffer from AF [3]. AF is not life-threatening, but it is associated with a variety of serious cardiovascular diseases, such as stroke and heart failure [4]. With the aggravating trend of aging population and increasing of factors inducing AF, AF will become a serious public health problem [5].

The traditional static electrocardiogram (ECG) has certain limitations for early detection and treatment of AF. Some patients with AF have no obvious clinical symptoms, and early AF always appears in a short time with no regular pattern (e.g., paroxysmal AF) [4]. Dynamic ECG monitoring has become a powerful tool for capturing AF and an effective method of automatic AF detection to deal with large amount of raw ECG data is needed. There are already lots of studies on the automatic detection algorithm of AF. These algorithms mainly focus on two aspects. One is the analysis of atrial electrical activity (e.g., the P wave disappears during AF and is replaced by a continuous irregular f wave.) [6] [7], another is the analysis of RR interval and heart rate variability [8]. The accuracy of these AF detection algorithms depends on the extraction of morphological features of ECG signals such as R wave, P wave or f wave. The detection accuracy will be significantly reduced if these features are missed or misused.

In recent years, the deep learning has developed rapidly, and has achieved considerable progress in the research fields such as image and speech processing. Recent studies indicate that the deep learning shows superior performance than traditional method. To overcome the limitations of traditional detection algorithms of arrhythmias, some researchers have begun to explore the application of deep learning methods to the detection of AF or other arrhythmias. Hannun, Awni Y., *et al.* used a 1-dimension convolutional neural network (1-D CNN) to classify 12 rhythm classes [9]. Yong Xia, *et al.* used short time Fourier transform (STFT) and a 2-D CNN to classify AF and sinus rhythm [10]. At present, due to the limited data set and the difficulty of ECG signal labeling, the research on ECG using deep learning method are still in its infancy. Nevertheless the research in this field is of great significance to human health and society.

In this study, a novel deep learning method to detect AF based on continuous wavelet transform (CWT) was proposed and it showed superior performance on public ECG database. Each segment of ECG signals has a fixed signal length of 10 s and was divided into one of the four classes: normal sinus rhythm (NSR), atrial fibrillation (AF), other types of arrhythmia except AF (OTHER), and noise signal (NOISE).

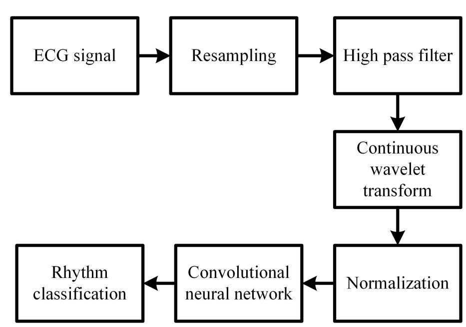


Fig. 1: Schematic of the proposed method.

This work was supported by the National Natural Science Foundation of China (61071004, 81671777), Shanghai Science and Technology Support Project (16441908300, 18441900900), Shanghai Municipal Science and Technology Major Project (2017SHZDZX01) and the Project of Shanghai Engineering Research Center (15DZ2251700).

Ziqian Wu and Xujian Feng are with the Department of Electronic Engineering, Fudan University, Shanghai, 200433, P. R. China.

* Corresponding author. Cuiwei Yang is with the Department of Electronic Engineering, Fudan University, Shanghai, 200433, P. R. China, and also with the Key Laboratory of Medical Imaging Computing and Computer Assisted Intervention of Shanghai, Shanghai Engineering Research Center of Assistive Devices, Shanghai, 200093, P. R. China (email: yangcw@fudan.edu.cn).

978-1-5386-1311-5/19/$31.00 ©2019 IEEE

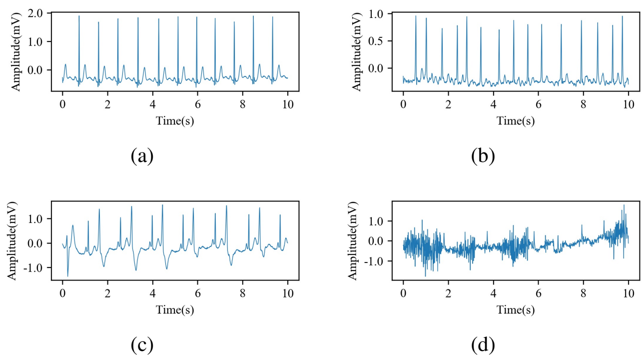


Fig. 2: Examples of each rhythm: (a) NSR, (b) AF, (c) OTHER, (d) NOISE.

First, CWT is performed on different scales to obtain the wavelet coefficient matrix with three wavelet bases used: the Mexican hat wavelet (Mexh), the Morlet wavelet (Morl) and the Complex Morlet wavelet (Cmor). Next, a CNN model was designed and then the wavelet coefficient amplitude matrix was used as input data of the CNN. Finally, the CNN is trained to classify 4 rhythms. The performance of the proposed method was evaluated by sensitivity, specificity, accuracy and receiver operating curve (ROC). The results showed that the proposed method performed better than many traditional AF detection algorithms.

## II. Methods and Materials

### A. Overview

Fig. 1 illustrates the schematic of the proposed method. The length of each ECG signal segment was fixed to 10 s, and each segment was resampled to 125 Hz due to the different sampling frequencies in different databases. A second order filter with a cut-off frequency of 0.5 Hz was applied to remove the baseline wander of each segment. After all this preprocessing, the continuous wavelet transform was performed to obtain the wavelet coefficient matrix of each segment. Then the wavelet coefficient amplitude matrix was normalized and was used for the input of the designed CNN. Finally, the CNN extracted the deep features of each segment and classified each segment.

### B. Data Seletion

We used multiple databases from different types of sensor to improve the robustness of the algorithm, so that the algorithm would adapt to a variety of measurement environments and conditions. These databases include the MIT-BIH Arrhythmia Database (DB1) [11], the MIT-BIH Malignant Ventricular Arrhythmia Database (DB2) [12], the MIT-BIH Atrial Fibrillation Database (DB3) [13], the Long-Term AF Database (DB4) [14], the MIT-BIH Normal Sinus Rhythm Database (DB5) [15] and the MIT-BIH Noise Stress Test Database (DB6) [16]. The ECG data in the first five databases were split into multiple data segments according to the rhythm annotation. In order to adapt the data to the input of the CNN, the length of ECG signal segment was set to a fixed length of 10 s, and signals with a rhythm duration less than 10 s were not used in this study. These

TABLE I: Distribution of data segments in each database

| Database | Rhythm | | | |
|---|---|---|---|---|
| | NSR | AF | OTHER | NOISE |
| **DB1** | 12014 | 1492 | 2336 | 0 |
| **DB2** | 3326 | 612 | 3666 | 0 |
| **DB3** | 99904 | 66964 | 1218 | 0 |
| **DB4** | 463810 | 421096 | 26542 | 0 |
| **DB5** | 250946 | 0 | 0 | 0 |
| **DB6** | 0 | 0 | 0 | 1080 |

TABLE II: Segment number and compositions of each rhythm

| Rhythm | Number | Compositions* |
|---|---|---|
| **NSR** | 4500 | NSR:4500 |
| **AF** | 4500 | AF:4500 |
| **OTHER** | 4350 | AFL:400, AB:500, B:500, T:200, IVR:10, VFL:40, VT:450, VFIB:60, VF:160, NOD:170, P:400, PREX:30, SBR:500, SVTA:450, BI:400, HGEA:80. |
| **NOISE** | 4500 | Data segments from DB6:1000, Simulated noise-contaminated signals:3500 |
| **Amount** | 17850 | |

* These abbreviations are standard rhythm annotation symbols from physionet.org [15].

segments were divided into 3 classes: NSR, AF, and OTHER. ECG signal often contains various noise components due to the presence of human respiration, myoelectric signals and noise from environment, so DB6 was used to add noise signals and generate ECG signals contaminated by noise. Standard noise data in DB6 including baseline wander (BW), muscle artifact (MA) and electrode motion artifact (EM) were split into data segments with the length of 10 s, and these segments were labelled as NOISE. Table I shows the different rhythms in each database. The noise data except BW were used to be added to the ECG signal, since the baseline has little influence on the morphological feature of ECG signals. Signals contaminated by noise were also labelled as NOISE. The rule of adding noise is defined as:

$$y = x + a * n \tag{1}$$

where $y$ is the signal contaminated by noise, $x$ is the raw ECG signal, $a$ is the gain of noise signal, $n$ is the noise signal. The value of $a$ is calculated by:

$$a = \sqrt{\exp(\frac{-\ln(10) * SNR}{10}) * \frac{S}{N}} \tag{2}$$

where $S$ is the power of raw ECG signal, $N$ is the power of noise signal, $SNR$ is the signal-to-noise ratio. The $SNR$ is set to -6 $db$ or -12 $db$ so that the morphological features of ECG signals were severely affected by noise and these signals cannot be interpreted by experts [17].

As showed in Table II, 4500 segments of NSR data, 4500 for AF were randomly selected from the first five databases, while 4350 for OTHER were manually selected due to its unbalanced data distribution. 1000 segments randomly selected from DB6 and 3500 simulated noise-contaminated signals constituted data labelled as NOISE. Fig. 2 shows the examples of each rhythm.

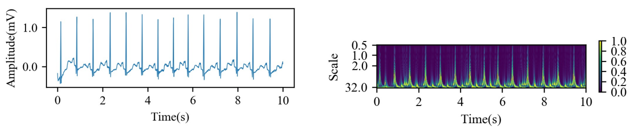


(a) (b)

Fig. 3: Result of CWT using Mexh wavelet: (a) ECG signal, (b) wavelet coefficient amplitude matrix.

### C. Continuous Wavelet Transform

CWT is a commonly used method of time-frequency analysis [18]. It reflects the frequency components of data changing with time. Time-frequency analysis can provide more information than the traditional time domain or frequency domain analysis. The CWT of sequence $x(t)$ is defined as:

$$W(a,b) = \int_{-\infty}^{+\infty} x(t)\frac{1}{\sqrt{a}}\psi(\frac{t-b}{a})dt \tag{3}$$

where $a$ is the scale factor and $b$ is the time shift factor, $\psi(t)$ is the function of wavelet basis. The scale can be converted to frequency by:

$$F = \frac{F_C * f_s}{a} \tag{4}$$

where $F_C$ is the center frequency of the wavelet basis, $f_s$ is the sampling frequency of signal.

Three kind of wavelet basis were used during the experiment.

- Mexh:

$$\psi(t) = \frac{2}{\sqrt{3}\sqrt[4]{\pi}}\exp(-\frac{t^2}{2})(1-t^2) \tag{5}$$

- Morl:

$$\psi(t) = \exp(-\frac{t^2}{2})\cos(5t) \tag{6}$$

- Cmor:

$$\psi(t) = \frac{1}{\sqrt{\pi B}}\exp(-\frac{t^2}{B})\exp(j2\pi Ct) \tag{7}$$

  where $B$ is the bandwidth of frequency response of the wavelet basis function, $C$ is the center frequency of the wavelet base.

The wavelet coefficient can be calculated by:

$$|W(a,b)| = \sqrt{W^2(a,b)} \tag{8}$$

In this study, the corresponding frequencies of the scales range from $f_s/(2*N)$ to $f_s/2$ (the Nyquist frequency) where $N$ is the number of scales. The frequency spacing was set to be uniform. Fig. 3 shows the result of CWT using Mexh wavelet.

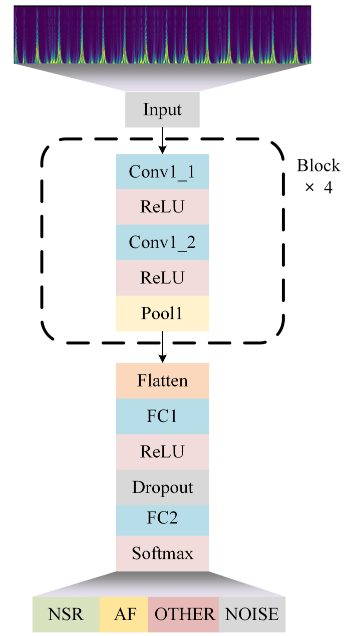


Fig. 4: Architecture of CNN.

### D. Architecture of Convolutional Neural Network

A common architecture of CNN in the field of deep learning is used in this study. The network contains three common network layers: convolutional layer, pooling layer and fully-connected layer. Fig. 4 illustrates the architecture of the network. Each part of the network is described as follows.

Input layer: Input of the CNN is a two-dimensional wavelet coefficient amplitude matrix, and the number of input channels is 1.

Block: Each block consists of two convolutional layers and one pooling layer. The parameters of the two convolutional layers are the same. The number of convolution kernels is 64, and the kernel size is 5×5 with a step size of 1 and an activation function of ReLU. After the convolution, a max pooling with a pool size of 2×2 is performed. The network uses four blocks to extract deep features of input matrix.

Fully connected layer: After the input matrix passes multiple convolution and pooling operations, all features are combined into one-dimensional features through the flatten layer, and then sent into the first fully connected layer, the first fully connected layer contains 128 neurons with an ac-

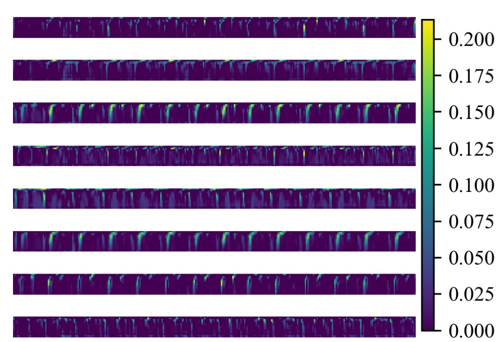


Fig. 5: Feature maps output by the second block.

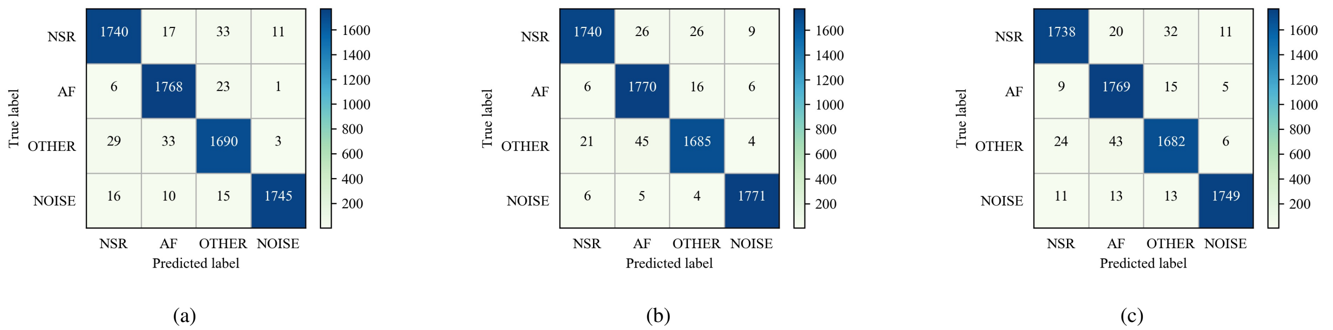


Fig. 6: Confusion matrices using different wavlet basis.

tivation function of ReLU. To prevent over-fitting and speed up the training process, a dropout layer with a dropout rate of 50% is added after the fully connected layer. Finally, the classification result is output through a fully connected layer with four outputs, and the activation function is softmax.

In this study, the loss function of the training process was cross entropy loss with an optimizer of root mean square prop (RMSprop). The initial learning rate, number of epochs and batch size were set to 0.0001, 50 and 32.

## III. RESULT

Fig. 5 shows 8 of the 64 feature maps output by the second block. Each feature map reflects the deep features abstracted from the primary features of the signal, reflecting the characteristics of the signal in the time-frequency domain from multiple levels, and is more comprehensive and detailed than the features extracted by the traditional methods. As the depth of the network increases, the features extracted by deep network become more complex and focus more on the global characteristics of the data [19]. The proposed method does not depend on the extraction of morphological features such as P waves or R waves, and avoids errors introduced by missed detection or false detection during processing.

For all the 17850 segments of selected ECG data, 60% of them (10710 segments) segments was selected as a training set, 40% of them (7140 segments) are used as the test set, and the proportions of each rhythm in training set and test set were the same. Fig. 6 shows the confusion matrices of the test set. The sensitivity and specificity for each rhythm are listed in Table III. Besides, the accuracy, average sensitivity, and average specificity for the whole test set are also listed.

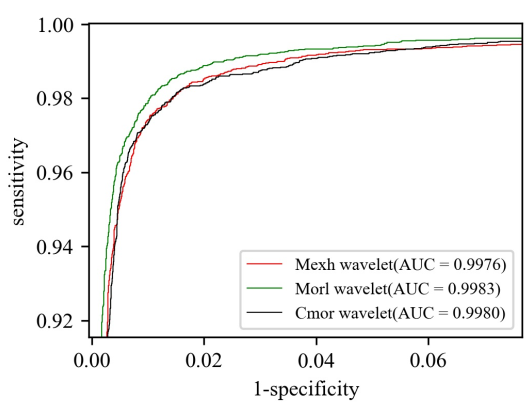


Fig. 7: ROCs of each classifier.

TABLE III: Performance of the proposed method.

| Performance | | Wavelet basis | | |
|---|---|---|---|---|
| | | **Mexh** | **Mor** | **Cmor** |
| **Accuracy** | | 97.24% | 97.56% | 97.17% |
| **Average sensitivity** | | 97.24% | 97.56% | 97.16% |
| **Average specificity** | | 99.08% | 99.19% | 99.06% |
| **Sensitivity** | **NORMAL** | 96.61% | 96.61% | 96.50% |
| | **AF** | 98.33% | 98.44% | 98.38% |
| | **OTHER** | 96.30% | 96.01% | 95.84% |
| | **NOISE** | 97.70% | 99.16% | 97.93% |
| **Specificity** | **NORMAL** | 99.04% | 99.38% | 99.18% |
| | **AF** | 98.88% | 98.58% | 98.58% |
| | **OTHER** | 98.68% | 99.15% | 98.89% |
| | **NOISE** | 99.72% | 99.65% | 99.59% |

The receiver operating curve (ROC) is used to evaluate the classifier. Fig. 7 shows the ROCs of each classifier using different wavelet bases, which all have good effects. The area under curve (AUC) values are: 0.9976 for the Mexh wavelet, 0.9983 for the Morl wavelet, 0.9980 for the Cmor wavelet. The best wavelet basis is Morl wavelet under the metrics including AUC value, accuracy, average sensitivity and average specificity.

## IV. DISCUSSION

The performance on AF detection of the proposed method was evaluated respectively. The sensitivity and specificity were 98.33% and 98.88% using the Mexh wavelet, 98.44%, 98.58% using the Morl wavelet, and 98.38%, 98.58% using the Cmor wavelet. Table IV shows the comparison between this work and previous studies. The performance of the proposed method was the best when both sensitivity and specificity were considered. Furthermore, this study was designed to classify 4 rhythms while previous studies was used to classify 2 rhythms: AF and NSR.

In particular, the proposed method does not depend on extraction of morphological features, avoiding the introduction of errors. Traditional methods such as analysis of HRV or RR interval may require data for a longer period of time, but in this study it only required a 10 s length ECG signal segment, which can greatly improve the work efficiency of doctors in clinic.

In addition to AF and NSR, two other rhythms were

TABLE IV: Comparison between this work and previous studies.

| Algorithm | Sensitivity | Specificity | Method | Databases |
|---|---|---|---|---|
| **Bruun** [20] | 96.51% | 99.19% | Discrete wavelet transform (DWT), HRV | DB1,DB3 |
| **Lee** [21] | 97.41% | 97.54% | Time-Varying coherence function, Shannon entropy | DB3,DB5 |
| **Dash** [22] | 94.4% | 95.1% | Variability of RR interval | DB1,DB3 |
| **Huang** [23] | 96.1% | 98.1% | Variability of RR interval | DB3,DB5 |
| **Xia** [10] | 98.34% | 98.24% | STFT, CNN | DB3 |
| **Proposed method (Mexh)** | 98.33% | 98.88% | CWT, CNN | DB1, DB2, DB3, DB4, DB5, DB6 |
| **Proposed method (Morl)** | 98.44% | 98.58% | CWT, CNN | DB1, DB2, DB3, DB4, DB5, DB6 |
| **Proposed method (Cmor)** | 98.38% | 98.58% | CWT, CNN | DB1, DB2, DB3, DB4, DB5, DB6 |

considered: NOISE and OTHER, which makes the proposed method meet more demand in practical applications. Moreover this study used data from multiple databases, taking into account the difference in signals that may be caused by various measurement conditions such as sensor types, measurement environment, and physical conditions of subjects. Overall, compared with other methods, the proposed method had better robustness and stability.

## V. CONCLUSION

This study described a novel deep learning method to detect AF based on CWT. The proposed method does not depend on the detection of morphological indicators such as R wave and P wave, and it has shown excellent results in multiple public databases. An accuracy of 97.56%, an average sensitivity of 97.56%, and an average specificity of 99.19% was achieved based on Morl wavelet. In conclusion, the proposed method is expected promising for clinical applications with follow-up studies to achieve more data to be evaluated.

## ACKNOWLEDGMENT

We would like to thank other students in the Electrophysiology and Pacing Laboratory of the Department of Electronic Engineering, Fudan University.

## REFERENCES

[1] R. F. Bosch, W. Kirch, J.-D. Theuer, D. Pittrow, A. Kohlhau Ss En, S. N. Willich, and H. Bonnemeier, "Atrial fibrillation management, outcomes and predictors of stable disease in daily practice: prospective non-interventional study," *International journal of cardiology*, vol. 167, no. 3, pp. 750–756, 2013.

[2] K.-L. Chien, T.-C. Su, H.-C. Hsu, W.-T. Chang, P.-C. Chen, M.-F. Chen, and Y.-T. Lee, "Atrial fibrillation prevalence, incidence and risk of stroke and all-cause death among chinese," *International journal of cardiology*, vol. 139, no. 2, pp. 173–180, 2010.

[3] M. Zoni-Berisso, F. Lercari, T. Carazza, and S. Domenicucci, "Epidemiology of atrial fibrillation: European perspective," *Clinical epidemiology*, vol. 6, p. 213, 2014.

[4] V. Fuster, L. E. Ryd E N, D. S. Cannom, H. J. Crijns, A. B. Curtis, K. A. Ellenbogen, J. L. Halperin, J.-Y. Le Heuzey, G. N. Kay, J. E. Lowe, and Others, "Acc/aha/esc 2006 guidelines for the management of patients with atrial fibrillation," *Europace*, vol. 8, no. 9, pp. 651–745, 2006.

[5] G. V. Naccarelli, H. Varker, J. Lin, and K. L. Schulman, "Increasing prevalence of atrial fibrillation and flutter in the united states," *The American journal of cardiology*, vol. 104, no. 11, pp. 1534–1539, 2009.

[6] P. E. Dilaveris, E. J. Gialafos, S. K. Sideris, A. M. Theopistou, G. K. Andrikopoulos, M. Kyriakidis, J. E. Gialafos, and P. K. Toutouzas, "Simple electrocardiographic markers for the prediction of paroxysmal idiopathic atrial fibrillation," *American heart journal*, vol. 135, no. 5, pp. 733–738, 1998.

[7] G. K. Andrikopoulos, P. E. Dilaveris, D. J. Richter, E. J. Gialafos, A. G. Synetos, and J. E. Gialafos, "Increased variance of p wave duration on the electrocardiogram distinguishes patients with idiopathic paroxysmal atrial fibrillation," *Pacing and Clinical Electrophysiology*, vol. 23, no. 7, pp. 1127–1132, 2000.

[8] J. Park, S. Lee, and M. Jeon, "Atrial fibrillation detection by heart rate variability in poincare plot," *Biomedical engineering online*, vol. 8, no. 1, p. 38, 2009.

[9] A. Y. Hannun, P. Rajpurkar, M. Haghpanahi, G. H. Tison, C. Bourn, M. P. Turakhia, and A. Y. Ng, "Cardiologist-level arrhythmia detection and classification in ambulatory electrocardiograms using a deep neural network," *Nature Medicine*, vol. 25, no. 1, p. 65, 2019.

[10] Y. Xia, N. Wulan, K. Wang, and H. Zhang, "Detecting atrial fibrillation by deep convolutional neural networks," *Computers in biology and medicine*, vol. 93, pp. 84–92, 2018.

[11] G. B. Moody and R. G. Mark, "The impact of the mit-bih arrhythmia database," *IEEE Engineering in Medicine and Biology Magazine*, vol. 20, no. 3, pp. 45–50, 2001.

[12] S. D. Greenwald, "The development and analysis of a ventricular fibrillation detector," Ph.D. dissertation, Massachusetts Institute of Technology, 1986.

[13] G. MOODY, "A new method for detecting atrial fibrillation using r-r intervals," *Computers in Cardiology*, pp. 227–230, 1983.

[14] S. Petrutiu, A. V. Sahakian, and S. Swiryn, "Abrupt changes in fibrillatory wave characteristics at the termination of paroxysmal atrial fibrillation in humans," *Europace*, vol. 9, no. 7, pp. 466–470, 2007.

[15] A. L. GOLDBERGER, "Physiobank, physiotoolkit, and physionet : components of a new research resource for complex physiologic signals," *Circulation*, vol. 101, no. 23, p. 215, 2000.

[16] G. B. Moody, W. Muldrow, and R. G. Mark, "A noise stress test for arrhythmia detectors," *Computers in cardiology*, vol. 11, no. 3, pp. 381–384, 1984.

[17] Q. Li, C. Rajagopalan, and G. D. Clifford, "A machine learning approach to multi-level ecg signal quality classification," *Computer methods and programs in biomedicine*, vol. 117, no. 3, pp. 435–447, 2014.

[18] L. Cohen, *Time-frequency analysis*. Prentice hall, 1995, vol. 778.

[19] M. A. Nielsen, *Neural networks and deep learning*. Determination press USA, 2015, vol. 25.

[20] I. H. Bruun, H. Sms, E. S. Poulsen, and S. Puthusserypady, "Automatic atrial fibrillation detection: A novel approach using discrete wavelet transform and heart rate variability," in *International Conference of the IEEE Engineering in Medicine & Biology Society*, 2017, pp. 3981–3984.

[21] J. Lee, D. Mcmanus, and K. Chon, "Atrial fibrillation detection using time-varying coherence function and shannon entropy," in *International Conference of the IEEE Engineering in Medicine & Biology Society*, 2011, pp. 4685–4688.

[22] S. Dash, K. H. Chon, S. Lu, and E. A. Raeder, "Automatic real time detection of atrial fibrillation," *Annals of biomedical engineering*, vol. 37, no. 9, pp. 1701–1709, 2009.

[23] C. Huang, S. Ye, H. Chen, D. Li, F. He, and Y. Tu, "A novel method for detection of the transition between atrial fibrillation and sinus rhythm," *IEEE Transactions on Biomedical Engineering*, vol. 58, no. 4, pp. 1113–1119, 2011.